3 RESULTS AND DISCUSSION

3.1. Cyclic Voltammetry

3.1.1. Cyclic Voltammetry of polyaniline in aqueous sulphuric acid

Qualitative observation

During cycling of potential, with sweep rate $50mVs^{-1}$, the counter electrode was also coated with the polymer. The colour of polyaniline formed changed at different potentials because of polyaniline having different structural states. Gases evolved from working electrode substrates of Platinum (Pt) and Platinised Titanium (PT) at about -200mV scanning from positive to negative (cathodic) potentials, and also at the counter electrode at the same potential but from negative to positive (anodic) direction. No gas evolution occurred when Tin dioxide (SnO_2) and Titanium (Ti) were used as the working electrode. The gas mentioned above was hydrogen, formed by the electrode reaction:

$$2H^+ + 2e^- = H_2$$

Polyaniline formed at the working electrode was powdery and green in colour and did not adhere very well on the surface of the working electrode.

Typical Cyclic Voltammogram of aniline in aqueous sulphuric acid

Figure 3.1 shows typical CV's for aniline on Platinum in sulphuric acid solutions. Five peaks found along oxidation and reduction directions indicate that materials occurred in redox pairs. Section (j) is caused by the hydrogen evolution where peak (a) corresponds to hydrogen desorption.

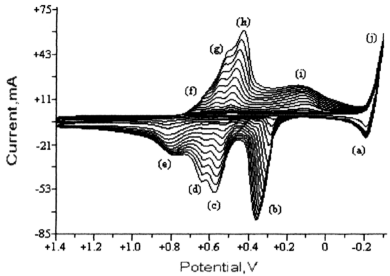

Figure 3.1 A typical Cyclic Voltammogram (CV) for aniline in sulphuric acid solutions.
Solution: - 0.1M aniline + 1.0M H_2SO_4
Working electrode: Platinum (Pt) with geometrical surface area = $0.97cm^2$
Number of sweeps: - (1-30) th
Sweep rate = $50mVs^{-1}$

Peak (b) corresponds to the oxidation reaction in the conversion of the leucoemeraldine form to the green conducting protonated emeraldine[51, 52, 54-56].

$$[-(C_6H_4)\text{-}N(H)\text{-}(C_6H_4)\text{-}N(H)\text{-}]_{4x}$$

$$\uparrow\downarrow \text{ (b)}$$

$$[-(C_6H_4)\text{-}N(H)\text{-}(C_6H_4)\text{-}N(H)\text{-}]_{3x}\text{--}[-(C_6H_4)\text{-}N^+(H)\text{=}(C_6H_4)\text{=}N^+(H)\text{-}]_x + 2xe^-$$

$$\uparrow\downarrow \text{ (c)}$$

$$[-(C_6H_4)\text{-}N(H)\text{-}(C_6H_4)\text{-}N(H)\text{-}]_{2x}\text{--}[-(C_6H_4)\text{-}N^+(H)\text{=}(C_6H_4)\text{=}N^+(H)\text{-}]_{2x} + 2xe^-$$

The peaks (c) and (d) involved further oxidation of dark green emeraldine form to partly or fully oxidised form of pernigraniline:

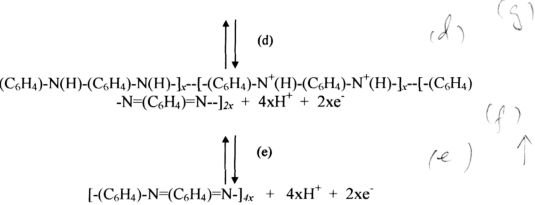

All the reactions shown above are apparently reversible, so that the peaks (f), (g), (h) and (i) would be due to the reductions of materials from peaks (e), (d), (b) and (c) respectively.

3.1.2 . Effect of concentration of monomer (aniline) on CV of PANI

Figure 3.2 shows a comparison between the solutions with and without aniline in 1.0M H_2SO_4. No peak growth was evident for the blank (no aniline) solution while polymerization occurred in the solution containing 0.1M aniline. Hydrogen desorption peaks were found in both the blank solution and the test solutions with Pt as working electrode. Comparison of polymerization rate was made using the heights of current peaks. 0.1M, 0.2M, 0.3M aniline in 1.0M H_2SO_4 produced different values of current peaks. Figure 3.3 showed that the CV's for higher concentration of aniline gave higher current peaks which could mean that polymerization occurred more rapidly at higher concentrations of aniline.

From figures 3.4 and 3.5, the current peaks for 0.2M aniline are higher than those for 0.3M after a fixed number of sweeps. Figure 3.6 shows the final results for three different solutions. From the comparison of the CV's for 0.1M and 0.2M or 0.3M aniline solutions, it is quite obvious that the polymerisation rate for 0.1M aniline was much lower and the amount of polyaniline produced was also found to be less for the same period of polymerisation time. Increasing the concentration of aniline from 0.2M to 0.3M did not result in advantageous increases on either polymerisation rate or the amount of polyaniline formed.

A limitation of current measurement was found after 20 sweeps in the 0.3M aniline + 1.0M H_2SO_4 solution or 13 sweeps in 0.3M aniline + 2.0M H_2SO_4 solution (Figure 3.6). This feature was caused by the inability of the BAS 100W instrument in measuring higher current in the CV mode (>200mA).

Similar results were obtained from a group of solutions containing 0.1, 0.2, 0.3M aniline in 2.0M sulphuric acid as shown in Fig. 3.7 and Figure 3.18. Figure 3.8 showed the same feature where higher concentration of aniline produced higher current peaks although the working electrode used was SnO_2.

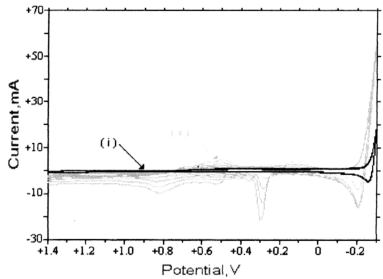

Figure 3.2 CV showing (1-10)th sweeps of solutions containing :-
(I) 1.0M H_2SO_4
(II) 1.0M H_2SO_4 + 0.1M aniline
Sweep rate = 50mVs^{-1}

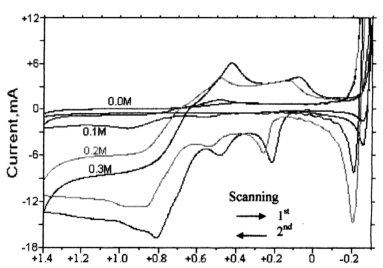

Figure 3.3 CV showing the current height is dependent on the concentration of aniline.
Number of sweeps: (1-2)th working electrode : Pt
Solutions conditions: - Different concentrations of aniline in 1.0M H_2SO_4
Sweep rate = 50mVs^{-1}

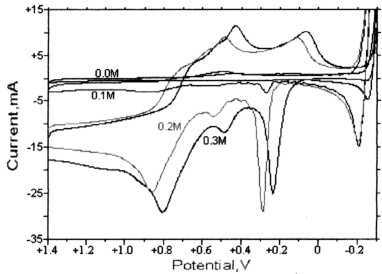

Figure 3.4 CV showing that the first oxidation peak of 4th sweep for 0.2M aniline is greater than that of 0.3M aniline.
Working electrode : Pt
Sweep rate = $50mVs^{-1}$

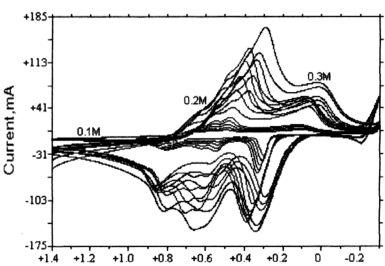

Figure 3.5 CV showing (11-20)th sweeps for different concentration of aniline in 1.0M H_2SO_4
Working electrode : Pt
Sweep rate = $50mVs^{-1}$

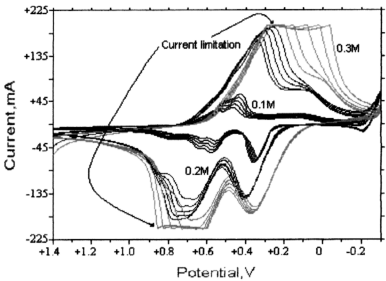

Figure 3.6 CV showing a limitation of current measured by the instrument
Solutions :- Different concentrations of aniline in 1.0M H_2SO_4
Working electrode :- Pt
Number of sweeps :- (21-30)th
Sweep rate = 50mVs^{-1}

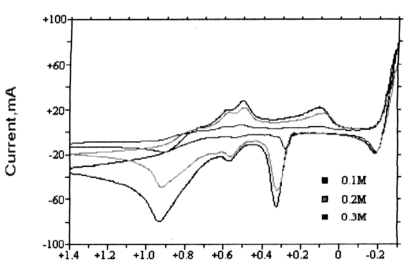

Figure 3.7 CV showing the effect of concentration of aniline on polymerisation rate in 2.0M H_2SO_4.
Solutions conditions :- 0.1M, 0.2M, 0.3M aniline in 2.0M H_2SO_4
Number of sweeps :- (3-4)th
Working electrode :- Pt
Sweep rate = 50mVs^{-1}

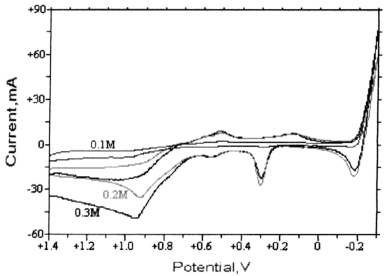

Figure 3.8 CV showing the effect of concentration of aniline on polymerisation rate in 2.0M H_2SO_4.
Solutions conditions :- 0.1M, 0.2M, 0.3M aniline in **2.0M** H_2SO_4
Number of sweeps :- **(1-2)th**
Working electrode :- Pt Sweep rate = $50mVs^{-1}$

Same feature as aniline in 1.0M H_2SO_4

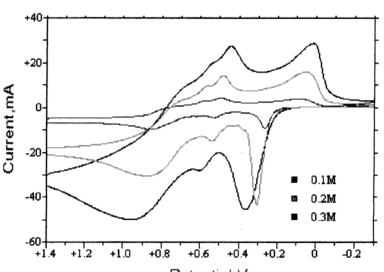

Figure 3.9 CV showing the effect of concentration of aniline on polymerisation rate in 1.0M H_2SO_4.
Solutions conditions :- 0.1M, 0.2M, 0.3M aniline in 1.0M H_2SO_4
Number of sweeps :- **(5-6)th**
Working electrode :- **SnO_2** Sweep rate = $50mVs^{-1}$

3.1.3. Cyclic Voltammetry of polyaniline on SnO_2 surface

The cyclic voltammogram given in figure 3.10 was typical for SnO_2 working electrodes. Peaks (1) to (4) corresponded to polyaniline in different forms as described in section 3.1.1. Peak (1) was shifted from less than +300mV to more than +500mV after 30 cycles of polyaniline growth. Peaks (2) and (3) were also shifted to higher positive potentials. As the oxidation peaks shifted, the reduction peaks (1', 2', 3', 4') moved to the more negative region of potentials. Peaks (2) and (3) almost overlap while peak (4) almost disappeared. All the reduction peaks tended to overlap after many sweeps (Figure 3.11). All the peaks appeared broader when SnO_2 was used as working electrode material.

No hydrogen evolution peaks were observed for the SnO_2 electrode.

The first oxidation peak (1) of polyaniline stopped growing after a certain number of sweeps (11 sweeps compared to 34 sweeps with Pt) as shown in figure 3.10. This feature indicated that the polymerisation of aniline stopped and the amount of polyaniline formed did not increase.

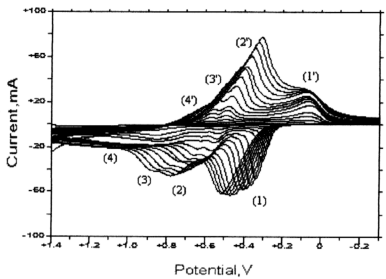

Figure 3.10 Cyclic Voltammogram of electropolymerisation of aniline in sulphuric acid solution with SnO_2 as working electrode.
Solution :- 0.1M aniline + 1.0M H_2SO_4
Working electrode :- SnO_2/Ti
Number of sweeps :- (1-30)th
Sweep rate = 50mVs^{-1}

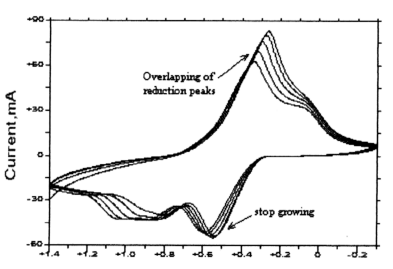

Figure 3.11 Cyclic Voltammogram of electropolymerisation of aniline in sulphuric acid solution with SnO_2 as working electrode.
Solution :- 0.1M aniline + 1.0M H_2SO_4
Working electrode :- SnO_2/Ti
Number of sweeps :- (61-70)th
Sweep rate = 50mVs^{-1}

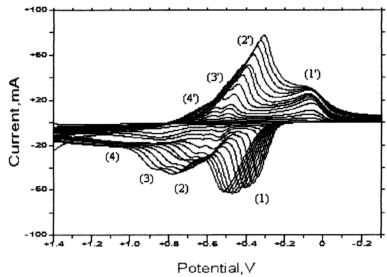

Figure 3.10 Cyclic Voltammogram of electropolymerisation of aniline in sulphuric acid solution with SnO_2 as working electrode.
Solution :- 0.1M aniline + 1.0M H_2SO_4
Working electrode :- SnO_2/Ti
Number of sweeps :- (1-30)th
Sweep rate = 50mVs^{-1}

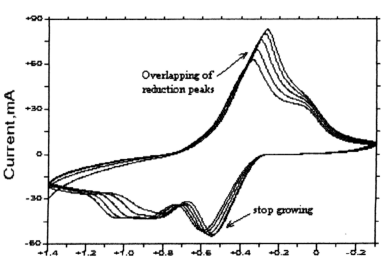

Figure 3.11 Cyclic Voltammogram of electropolymerisation of aniline in sulphuric acid solution with SnO_2 as working electrode.
Solution :- 0.1M aniline + 1.0M H_2SO_4
Working electrode :- SnO_2/Ti
Number of sweeps :- (61-70)th
Sweep rate = 50mVs^{-1}

3.1.4. The differences between Pt and SnO_2 as working electrode

The CV's for commencement of 1 to 10 cycles polymerisation of aniline on Pt and on SnO_2 are shown in figures 3.12 and 3.13. The first oxidation peaks for both electrodes are higher than second, third and fourth oxidation peaks. The potentials where those peaks were found were almost identical for polyaniline formation on both types of electrode substrate. In the case of Pt, where hydrogen evolution reaction (h.e.r.) occurred, the hydrogen desorption peak was very distinct on the reverse sweeps. The feature was obviously absent for the case of SnO_2 where no h.e.r. was observed.

As the polyaniline kept on growing, the all the oxidation and reduction peaks overlapped except the first oxidation peak. This peak for the case of SnO_2 remains higher than other peaks (in the current height, Figure 3.15). But the growth of the same peak was slowed down in the case of Pt. The overlapping peak is higher than it as shown in the figure 3.14.

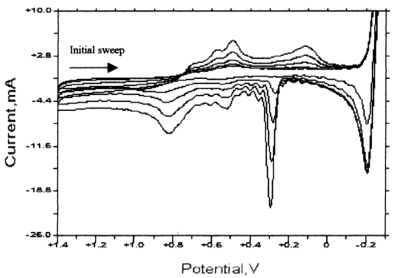

Figure 3.12 Cyclic Voltammogram of electropolymerisation of aniline in sulphuric acid solution with Pt as working electrode.
Solution :- 0.1M aniline + 1.0M H_2SO_4
Working electrode :- Platinum
Number of sweeps :- (1-10)th Sweep rate = $50mVs^{-1}$

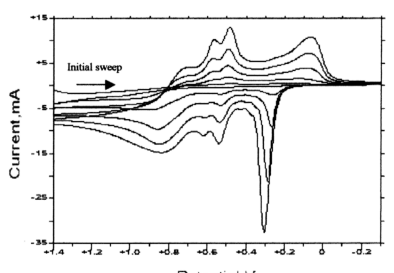

Figure 3.13 Cyclic Voltammogram of electropolymerisation of aniline in sulphuric acid solution with SnO_2 as working electrode.
Solution :- 0.1M aniline + 1.0M H_2SO_4
Working electrode :- SnO_2/Ti
Number of sweeps :- (1-10)th Sweep rate = $50mVs^{-1}$

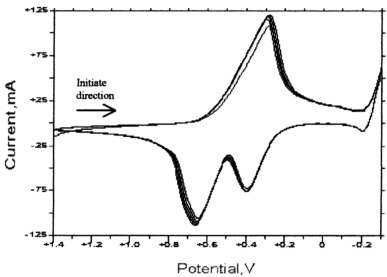

Figure 3.14 Cyclic Voltammogram of electropolymerisation of aniline in sulphuric acid solution with Pt as working electrode.
Solution :- 0.1M aniline + 1.0M H_2SO_4
Working electrode :- Platinum
Number of sweeps :- (51-60)th
Sweep rate = 50mVs^{-1}

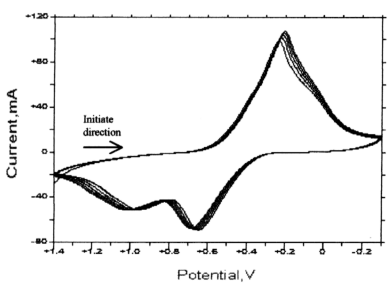

Figure 3.15 Cyclic Voltammogram of electropolymerisation of aniline in sulphuric acid solution with SnO_2 as working electrode.
Solution :- 0.1M aniline + 1.0M H_2SO_4
Working electrode :- Stanum dioxide
Number of sweeps :- (51-60)th
Sweep rate = 50mVs^{-1}

3.1.5. Cyclic Voltammetry of polyaniline by Ti

Experiments showed that titanium was not very electrocatalytically active in the electropolymerization of aniline, as indicated by the slow reaction of the polyaniline formations. No polymerisation peaks were observed during the first 10 sweeps of the cyclic voltammogram shown in the figure 3.16.

(1-80) th sweeps are given in figure 3.17 where only two peaks were found in the cyclic voltammogram of oxidation of polyaniline in sulphuric acid solution. The first oxidation peak occurred in the potential range +400 to +600mV. This peak corresponds to peak (a) and peak (1) for the electropolymerization of aniline on platinum and tin dioxide respectively. The peak current was lower than for the other oxidation peaks. Another broad peak (from +600 to +1100mV) was the result of overlapping of peaks 2, 3 and 4.

The number of reduction peaks is equivalent to the oxidation peaks. The reduction peak 1' occurred at -150mV is higher than the rest reduction peaks.

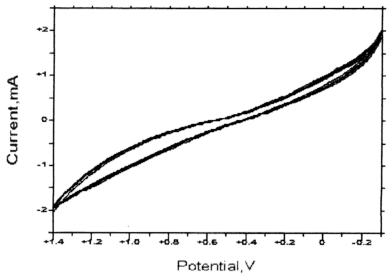

Figure 3.16 Cyclic Voltammogram of electropolymerisation of aniline in sulphuric acid solution with Ti as working electrode.
Solution :- 0.1M aniline + 1.0M H_2SO_4
Working electrode :- Titanium
Number of sweeps :- (1-10)th
Sweep rate = 50mVs^{-1}

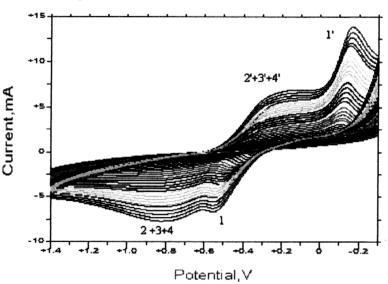

Figure 3.17 Cyclic Voltammogram of electropolymerisation of aniline in sulphuric acid solution with Ti as working electrode.
Solution :- 0.1M aniline + 1.0M H_2SO_4
Working electrode :- Titanium
Number of sweeps :- (1-80)th
Sweep rate = 50mVs^{-1}

3.1.6. Effect of concentration of sulphuric acid on polymerisation of polyaniline.

CV's in 1.0M and 2.0M H_2SO_4 solutions were compared, with the more concentrated acid showing an enhancement on polymerisation rate of aniline. Current peaks for 2.0M acid solution were higher than 1.0M acid as showed in figure 3.18. The results support the contention that the polymerization of aniline involved the aniline cation radical which existed in the acidic medium.

As mentioned in section 3.1.2, a higher concentration of monomer aniline enhanced the electropolymerization of aniline in 1.0M or 2.0M H_2SO_4. Figure 3.8 in section 3.1.2 showed the effect of aniline concentration on the Cyclic Voltammogram.

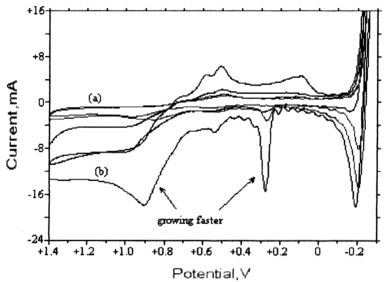

Figure 3.17 CV showing the faster growth of polyaniline in higher concentration of sulphuric acid.
Solutions :- 0.1M aniline + **1.0M** H_2SO_4 (a)
0.1M aniline + **2.0M** H_2SO_4 (b)
Number of sweeps :- (1-4)th
Working electrode :- Pt

3.1.7. Polymerisation at various working electrodes

The purpose of this part of the experiment is to investigate the polymerisation rates and the reactions involved by using different working electrode substrates.

The cyclic voltammograms differ in shape for different electrode materials. A series of cyclic voltammograms was listed in the Appendix 4. Among the four types of working electrode surfaces, Pt and PT were seen to be similarly electrocatalytically active in the electropolymerization of aniline: -

$$Pt \sim PT > SnO_2 > Ti$$

The CV for Pt and PT are similar in terms of peak currents and peak potentials. From the CV shown at Figure 3.18, sintered PT showed a compatible value of current height to Pt. SnO_2 gave oxidation peaks slightly lower than both Pt and PT but they were generally much higher than those obtained with Ti (Figure 3.21). Besides lower current, CV's for SnO_2 also appeared to have somewhat different shapes, where the peaks for oxidation and reduction of polyaniline were shifted and no hydrogen desorption peaks were found. According to figure 3.19, oxidation potentials for peaks (a) and (b) of polyaniline on Pt were +380 and +600mV respectively but they were shifted to +550(a') and +900mV(b') in the case of SnO_2. For reduction peaks (c) and (c'), they differed by about 140mV(shifted from +400mV to +260mV). The first oxidation peak in CV of Ti only appeared after 20 sweeps (Figure 3.20). The overall comparison of four types of working electrodes is shown at figure 3.21.

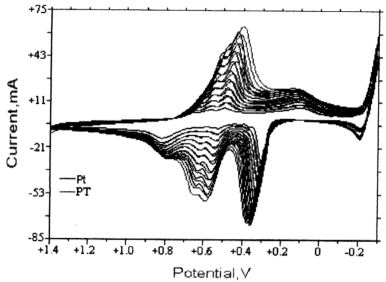

Figure 3.18 CV showing compatible value in current peak heights for Pt and PT as working electrodes
Solution :- 0.1M aniline + 1.0M H_2SO_4
Number of sweeps :- (11-30)th
Sweep rate = 50mVs^{-1}

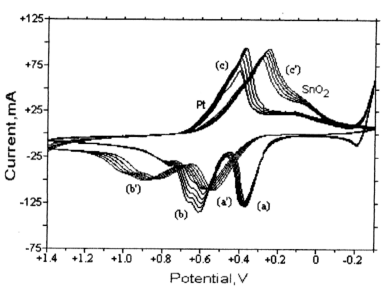

Figure 3.19 CV showing that oxidation peaks of polyaniline on Pt is higher than for SnO_2 but the shapes are different.
Solution :- 0.1M aniline + 1.0M H_2SO_4
Number of sweeps :- (31-40)th
Sweep rate = 50mVs^{-1}

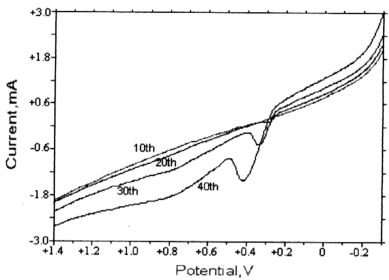

Figure 3.20 CV showing the first oxidation peak of polyaniline on Ti occurred after 20^{th} sweeps.
Solution :- 0.1M aniline + 1.0M H_2SO_4
Working electrode :- Ti
Sweeps :- 10, 20, 30, 40th
Sweep rate = $50mVs^{-1}$

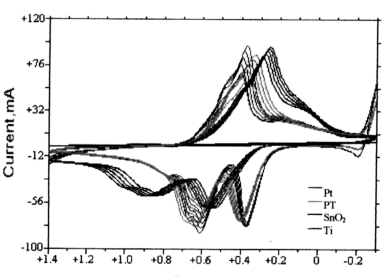

Figure 3.21 CV showing overall view of difference in current height for different types of working electrode used.
Solution :- 0.1M aniline + 1.0M H_2SO_4
Number of sweeps :- (31-40)th
Sweep rate = $50mVs^{-1}$

3.1.8. Incorporation of Orthanilic acid into polyaniline

A primary object of this project is to seek to apply conducting polymers in wastewater treatment, especially in heavy metals removal. In order to use ion-exchange techniques for extraction of heavy metals by using polyaniline, cationic ion exchangers must be introduced into the material itself. Orthanilic acid is used for supplying sulphonic groups (SO_3^-) into the polymer matrix. Orthanilic acid has the molecular structure:

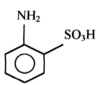

3.1.9. Effect of adding orthanilic acid to the Cyclic Voltammetry of Polyaniline

With the introduction of orthanilic acid to the solutions of aniline in sulphuric acid, it was observed that the polymerisation rate of aniline decreased. Sulphonation of polyaniline with orthanilic acid led to the formation of a polymeric composite of both polymerized aniline and orthanilic acid which was soluble in dilute alkali solutions. The results from microanalysis showed that the ratio of S to nitrogen atom in sulphonated polyaniline was 1: 4 (Appendix 2).

It is clear that from figure 3.22, the polymerisation rates of solutions containing orthanilic acid were low. Further increases in concentration of orthanilic acid even prohibit the polymerisation.

Overlapping of oxidation peaks was found in the presence of orthanilic acid. The first oxidation peak was not affected except for the value of current obtained (Figure 3.23).

J. Y. LEE [7, 16] had carried out the sulphonation by using methanilic acid instead of orthanilic acid. The polyaniline-like structure of PAN-methanilic acid was ascertained. As mentioned above the conductivity of copolymer decrease with the presence of sulphonate groups. Both polyaniline-orthanilic acid and polyaniline-methanilic acid were soluble in alkaline solvent (0.1M NaOH).

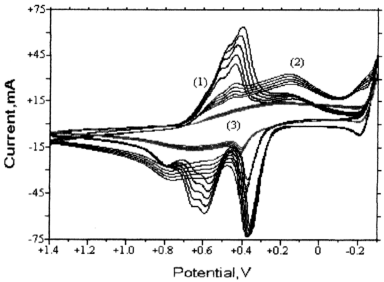

Figure 3.22 CV showing effect of adding orthanilic acid into electrolytes
Solutions :- (1) 0.1M aniline + 1.0M H_2SO_4
(2) 0.1M aniline + **0.01M orthanilic acid** + 1.0M H_2SO_4
(3) 0.1M aniline + **0.05M orthanilic acid** + 1.0M H_2SO_4
Number of sweeps :- (21-30)th
Working electrodes :- PT
Sweep rate = 50mVs^{-1}

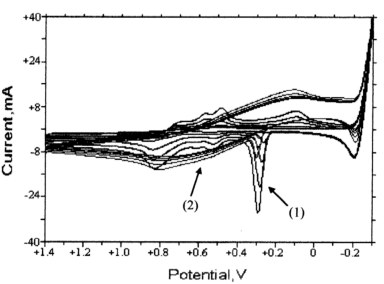

Figure 3.24 CV showing the difference between solutions with and without orthanilic acid.
Solutions :- (1) 0.1M aniline + 1.0M H_2SO_4
(2) 0.1M aniline + 0.01M orthanilic acid + 1.0M H_2SO_4
Working electrode :- PT
Number of sweeps :- (1-10)th
Sweep rate = 50mVs^{-1}

3.1.10. Thermal effect

In the solutions containing 0.05M aniline, 0.05M orthanilic acid and 1.0M surphuric acid, an obvious enhancement on polymerisation rate was found initially as the temperature was increase from 25° to 50°C (Figure 3.24). But after a number of sweeps (about 40), the current values were nearly the same (Figure 3.25) for both 25°C and 50°C. More aniline monomers were polymerised at the beginning of the reaction under 50°C, but as polymerisation proceed, the total amount of polyaniline formed was about the same. The total amount of polyaniline produced was strongly affected by the concentration of monomeric aniline present in solution. Figure 3.25 showed that the first oxidation peak was shifted to more anodic (from +300mV to +450mV) region when higher temperature was applied.

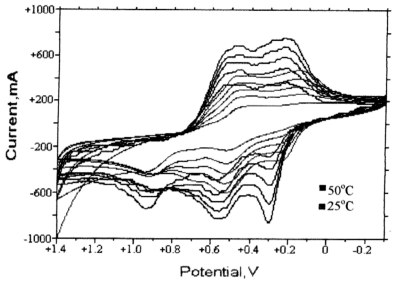

Figure 3.24 CV showing the effect of temperature to the co-polymerisation of aniline and orthanilic acid
Solutions :- 0.05M aniline + 0.05M orthanilic acid + 1.0M H_2SO_4
Number of sweeps :- **(1-10)**th
Working electrodes :- SnO_2
Sweep rate = $50mVs^{-1}$

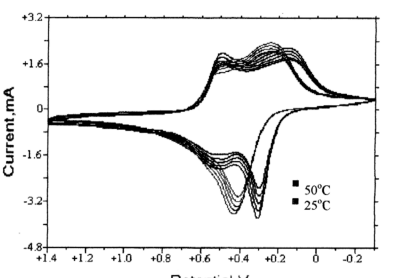

Figure 3.25 CV showing the effect of temperature to the co-polymerisation of aniline and orthanilic acid
Solutions :- 0.05M aniline + 0.05M orthanilic acid + 1.0M H_2SO_4
Number of sweeps :- **(31-40)**th
Working electrodes :- SnO_2
Sweep rate = $50mVs^{-1}$

3.1.11. Quantitative Analysis

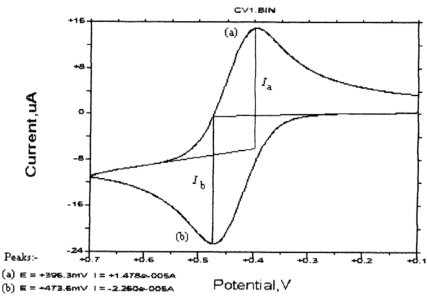

Figure 3.26 Peaks coordinate showed in a Cyclic Voltammogram

The value of currents was obtained from the Cyclic Voltammogram using the BAS 100W program. Figure 3.26 shows how values of peaks current and potential were recorded. The parameters of peak (a) and (b) are shown at left bottom corner of the graph.

Some peaks overlapped after a certain number of sweeps; so only three peaks were compared. They were the two oxidation peaks (1 and 2) and the reduction peak (3) (Figure.3.27). From figure 3.28, the polymerization reached a maximum, which is not because of the instrument limitation but the amount of the aniline in the sample solution. The polymerization began at a slower rate and followed by rapid formation of polyaniline before reaching the limiting state, which occurred at both oxidation (Figures 3.28 and 3.29) and reduction peaks (Figure 3.30).

The performance of electrodes was compared in figure 3.31 to figure 3.33. Titanium has poorest activity among the electrodes used. Although the first oxidation peak was comparable to those for Pt and PT, SnO_2 showed lower activity in the second oxidation peak as well as the reduction peak.

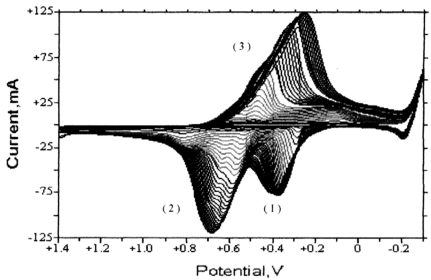

Figure 3.27 CV showing three peaks in the consideration of peak current values for comparison for electropolymerisation of aniline on different working electrodes

(1) The first oxidation peak
(2) The second oxidation peak
(3) The reduction peak

Table 3.1 : Current values for first oxidation peak in the solutions containing different concentration of aniline on Pt surface.

No. sweeps	Peak Current / mA		
	0.1M ani / 1.0M H_2SO_4	0.2M ani / 1.0M H_2SO_4	0.3M ani / 1.0M H_2SO_4
2	0.6987	5.371	7.642
6	7.904	49.91	40.39
10	21.44	70.22	81.88
14	41	118	108.1
18	55.2	130.5	140.8
22	64.63	138.1	160.5
26	71.18	142	169.2
30	74.67	146.5	173.6
34	77.84	148.1	193.3
38	78.06	151.8	196.4
42	77.46	150.7	
46	76.74	156.6	
50	75.66	160.1	
54	75.78	153.4	
58	75.78	154.2	
62	75.78		

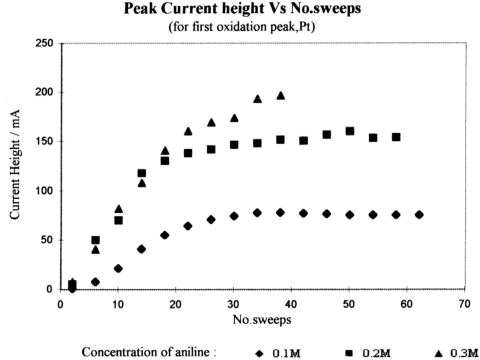

Figure 3.28 Plot showing the current value as the no. sweeps increases for solutions containing different concentrations of aniline on Platinum surface

Table 3.2 : Current values for second oxidation peak in the solutions containing different concentrations of aniline on Pt surface

No. sweeps	Peak Current / mA		
	0.1M ani / 1.0M H_2SO_4	0.2M ani / 1.0M H_2SO_4	0.3M ani / 1.0M H_2SO_4
2	0.9684	4.961	5.852
6	2.672	16.49	19.83
10	5.686	35	46.03
14	11.45	65.44	82.45
18	21.38	100.8	120.9
22	31.86	146.7	187.2
26	43.39	170	204.5
30	54.92	185.8	
34	70.11	195.2	
38	79.72	199.9	
42	88.94	205.4	
46	96.24		
50	102.4		
54	108.9		
58	112.7		
62	115.2		
66	117.5		
70	119.2		

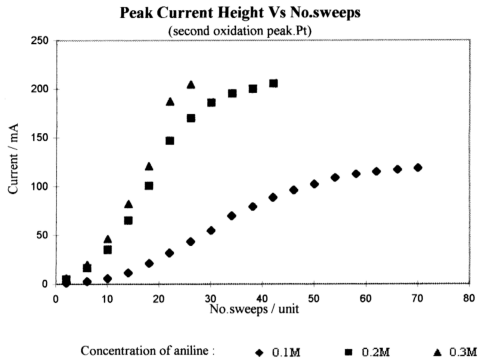

Figure 3.29 Plot showing the current value as the no. sweeps increases for solutions containing different concentrations of aniline on Platinum surface

Table 3.3 : Current values for second oxidation peak in the solutions containing different concentrations of aniline on Pt surface

No. sweeps	Peak Current / mA		
	0.1M ani / 1.0M H_2SO_4	0.2M ani / 1.0M H_2SO_4	0.3M ani / 1.0M H_2SO_4
1	1.638	4.323	6.079
5	2.686	17.58	19.44
9	5.306	35.05	47.74
13	10.85	68.33	92.78
17	20.98	114.5	127.7
21	32.86	165.8	195.4
25	46.15	183.9	
29	60.12	192	
33	76.64	192.5	
37	89.61	196	
41	99.63		
45	106.7		
49	112		
53	115.4		
57	119.6		
61	121.5		
65	123.2		
69	124.4		

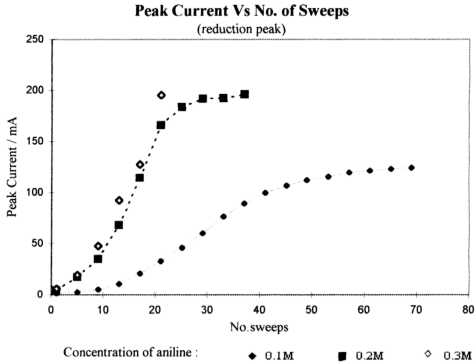

Figure 3.30 Plot showing the peak current value increased as the no. sweeps increases for solutions containing different concentrations of aniline on Platinum surface.

Table 3.4 : Current values for first and second oxidation peaks on different types of working electrodes

	First oxidation peak				Second oxidation peak		
No.sweeps	Ti	PT	Pt	SnO_2	PT	Pt	SnO_2
2		0.833	0.6944	0.222	0.899	0.9722	0.444
6		11.39	7.917	9.111	3.333	2.639	4.444
10		29.39	21.53	32.1	7.889	5.694	12.78
14		48.6	41.4	54	15.78	11.46	23.48
18	0.1555	60	56	57.6	25.5	21.33	32.64
22	0.0667	69.8	65.2	62.8	38.64	32	37.08
26	0.1889	72.8	71.2		48.57	43.5	42.5
30	0.4611	73.4	74.6		58.1	55	45.69
34	0.7917	73.6	77.6		65.68	70.22	48.89
38	1.208	73.2	78		74.39	79.78	49.5
42	1.542	71.33			76	88.89	
46	1.917	75.5			86.67	96.22	
50	2.292	76.17			94	102.4	
54	2.708				95.11	109.1	
58	3.292				102	112.7	
62						115.1	
66						117.6	
70						119.1	

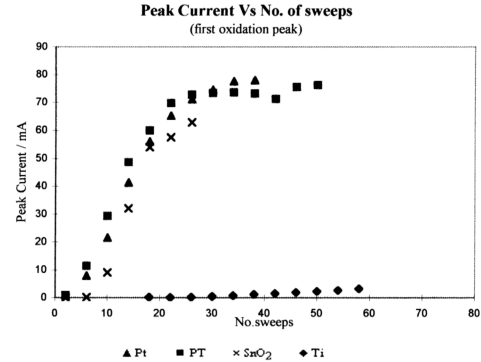

Figure 3.31 Plot showing the increment of the current value at first oxidation peaks for different working electrodes in the electropolymerisation of 0.1M aniline in 1.0M H_2SO_4

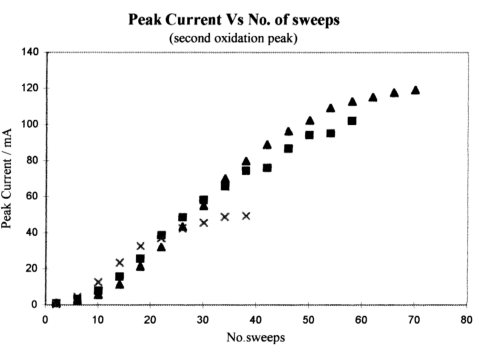

Figure 3.32 Plot showing the increment of the current value at second oxidation peak for different working electrodes in the electropolymerisation of 0.1M aniline in 1.0M H_2SO_4

Table 3.5 : Current values for reduction peaks on different types of working electrodes

	Peak Current / mA			
No.sweeps	Ti	Ptti	Pt	SnO_2
1		0.833	1.556	0.5
5		2.917	2.222	4.333
9		7.583	5.333	13
13		1.517	10.89	25.17
17		25.4	20.89	42.17
21	1.567	39.2	32.67	51.6
25	1.667	52	46	67.4
29	1.958	64	60.22	77.2
33	2.342	70	76.44	86.99
37	2.818	81.8	89.33	91.94
41	3.514	72.2	99.23	
45	4.138	90.97	106.8	
49	4.972	99.37	112.1	
53	5.667	92.81	115.4	
57	6.625	103.5	119.6	
61			121.4	
65			123.4	
69			124.7	

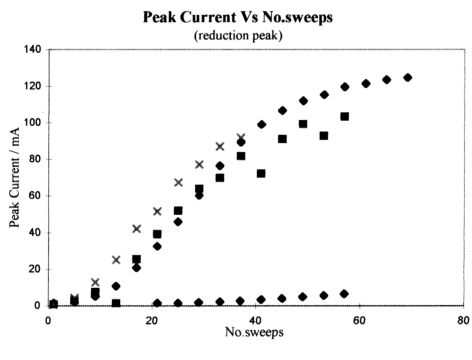

Figure 3.33 Plot showing the increment of the current value at first reduction peaks for different working electrodes in the electropolymerisation of 0.1M aniline in 1.0M H_2SO_4

3.2. Polypyrrole

Polyaniline is powdery and not easily amenable for film preparation. A conductive polyaniline film with conductivity 20 S cm^{-1} had been prepared composited on a non-conducting and flexible Poly (methyl methacrylate) layer [12]. The method was tried in this project but the author was not able to obtain nice, uniformly dispersed films. Only a limited amount of polyaniline was found at some spots on the PMMA layer after a long period of polymerisation.

Polypyrrole has better processibility compared to polyaniline. Free standing films, with good mechanical properties can be prepared easily. The application of polypyrrole in wastewater technology was reported recently [89].

3.2.1. Electropolymerization of pyrrole

Preparation of polypyrrole doped with large anions of polystyrene sulphonic acid (PSS) was carried out. The cyclic voltammogram of 0.5M pyrrole in 0.5M PSS on Pt is given in figure 3.35. No peak was found after many sweeps but the current was still growing slowly. This was probably because the surface area of the working electrode used was too large. The same characteristic was observed when Pt was replaced by Ti as working electrode. Figure 3.36 shows the first 10 sweeps for Ti. Ti as working electrode gave lower observed current compared to Pt.

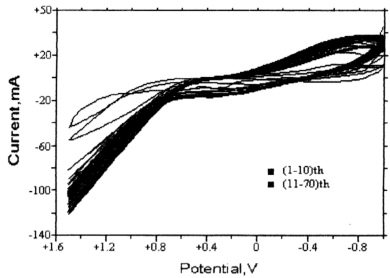

Figure 3.35 CV showing the 70 sweeps of electropolymerization of pyrrole
Solution :- 0.5M pyrrole + 0.5M Poly(styrene sulphonic) acid
Working electrode :- PT

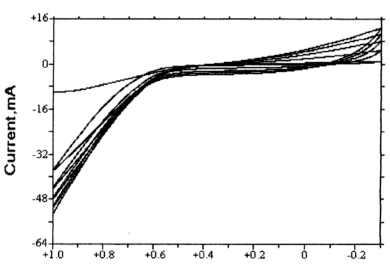

Figure 3.36 CV showing the electropolymerization of pyrrole on Titanium
Solution :- 0.5M pyrrole + 0.5M Poly(styrene sulphonic) acid
Working electrode :- Ti
Number of sweeps :- (1-10)th

3.2.2. Insertion of cation and anion in Ppy-PSS film [90, 91]

A Cyclic Voltammetry study on a pre-coated Polypyrrole film on Platinum as working electrode was carried out using 0.1M Sodium Perchlorate ($NaClO_4$) as electrolyte medium. Insertion of cation (Na^+) or anion (ClO^-_4) into the Ppy-PSS film can be inferred from the cyclic voltammogram. Figures 3.37 and 3.38 showed the difference in C.V. for two polymer films Ppy-PSS and Ppy-ClO_4. For Ppy-ClO_4 film, small dopant ClO^-_4 can be easily moved in and out of the polypyrrole matrix but large dopant, PSS is hardly released from polypyrrole. The redox peaks for polypyrrole in Ppy-PSS is slightly lower than for Ppy-ClO_4.

The amount of ion inserted was increased when higher scan rate was applied. Figure 3.37 shows the C.V. of ion insertion on Ppy-ClO_4 film for different scan rates from 10 to 200mVs^{-1}. The same feature was found in the case of Ppy-PSS film, which is shown, in Figure 3.38.

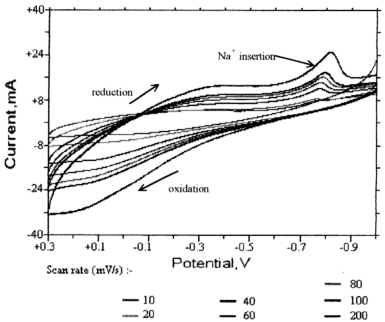

Figure 3.37 CV showing the insertion of Na^+ cation into the Ppy-ClO_4 film.
Solution :- 0.1M $NaClO_4$
Working electrode :- **Ppy-ClO_4** on Pt
Number of sweeps :- (1-2)th

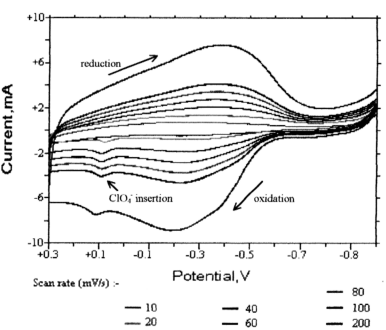

Figure 3.38 CV showing the insertion of ClO_4^- anion into Ppy-PSS film.
Solution :- 0.1M $NaClO_4$
Working electrode :- **Ppy-PSS** on Pt
Number of sweeps :- (1-2)th

3.2.3. **Conductivity**

Materials suitable as insulators require high electrical and thermal resistivity. On the other hand, conductors should possess high conductivities for optimum performance. Polymeric materials e.g. polypropylene (with electrical resistivity > 10^{15} Ωm^{-1}) and Nylon 6,6 (10^{12}-10^{13} Ωm^{-1}) were suitable for making insulators. Copper is a good conductor because of its very high conductivity, 6.0×10^{17} S m^{-1}. Semiconductors e.g. germanium and silicon which are used for making diodes and transistors possess conductivities which fall between insulators and conductors.

Understanding the mechanisms of charge transfer in conducting polymers is becoming very important as such materials have many potential applications. Conducting polymers normally have highly conjugated π system, and this is believed to be the main reason for its electrical conductivity. Recently a lot of composites [3-31] between conducting polymers and other polymeric materials (conducting or non-conducting) were synthesised with the aim of increasing physical material strength and conductivity. Such composites may contain moveable ions from the additives, and conducting mechanisms become more complicated.

The conductivities of undoped polymers (pristine) can be transformed from insulating to metallic by doping with electrolytes, conductivity increasing as the doping level increases [92]. The doping process can be carried out easily by electrochemical methods. The dopants (molecules and ions) are located between the matrix of polymer chains. They can donate charge to or accept charge from the polymer backbone. The polymer backbone and dopants may form new structures. There is a great variety in these structures, with different structures forming with different doping levels, different

processing routes and different dopants. For example, in the case of polypyrrole, different dopant levels can lead to different conductivities as shown in table 2 below:

Table 2: Effect of different doping level of BF_4^- anion to the conductivity of polypyrrole[92]

sample	% BF^-_4	Conductivity (S cm^{-1}) at 300K
PPY	6.5	$3.41x10^{-4}$
PPY	6.1	$2.33x10^{-4}$
PPY	5.0	$1.36x10^{-4}$

3.3. **Conductivity of Ppy-PSS**

3.3.1. Surface Conductivity Versus Film Thickness

Different thicknesses of Ppy-PSS films were prepared. See appendix 5 for the details of preparation. Using the method of "four-point probe", the surface conductivity was found to be dependent on the thickness of the films. Figures 3.39 and 3.40 show the variation of surface conductivity with thickness for films of different thicknesses (23.6 to 84μm). Conductivity changed significantly with thickness.

The conductivity of both sides of an electrolytically prepared polymer film were being compared and the results given in table 3.7 below:

Table 3.7: Comparison of surface conductivity for both electrolyte and electrode sides of Ppy-PSS film.

	Surface Conductivity / S m^{-1}		Percentage of differences
Thickness / μm	Electrolyte side	Electrode side	%
8.2	0.64	0.64	0.5
13.0	0.37	0.36	1.5
53.9	6.23	6.28	0.8
65.0	7.47	7.20	3.6

"Electrode side" refers to the surface originally attached to the metal electrode surface and "electrolyte side" refers to the film surface, which was facing the electrolyte during electropolymerization (For surface morphology, see appendix 6).

The results from Table 3.7 showed no significant difference in the surface conductivity of both sides of the films.

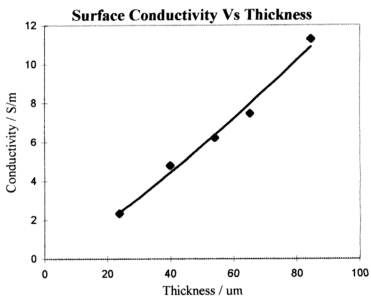

Figure 3.39 A plot of surface conductivity versus the thickness of Ppy-PSS films
(mw. PSS = 70,000)

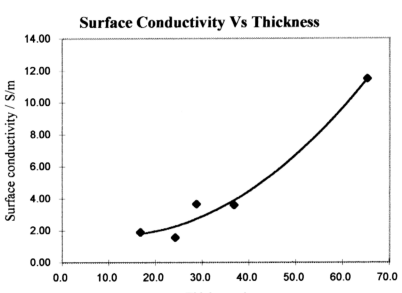

Figure 3.40 A plot of surface conductivity versus the thickness of Ppy-PSS films
(mw. PSS = 100,000)

3.3.2. **Calculation for surface conductivity**

According to Smits [75], in the method of "four-point probe" for measuring the resistivity of sheet materials, the resistivity is given by:

$$\textbf{Resistivity}, \rho = \textbf{(V/I) x C'} \qquad \ldots\ldots(3.3.2\ a)$$

where, V = potential measured, V

I = current measured, A

C' = Correction factor, cm

$$\textbf{Conductivity}, \sigma = \textbf{1/}\rho \qquad \ldots\ldots(3.3.2\ b)$$

$$= I / (V \times C')$$

$$= (I/V) / C'$$

$$\delta\sigma/\sigma = [\ \delta\,(I/V)\ ] / (I/V) \ + \ \delta\,C'/C'$$

An example of the calculation is given in Appendix 7.

Figure 3.41 showing the relationship between correction factor, C' and d/s value.

Table 3.8 The Correction Factor C' used for the method of "four-point probe" [78]

d/s	C' / cm
3.0	2.2662
4.0	2.9280
5.0	3.3625
7.5	3.9273
10.0	4.1716
15.0	4.3646
20.0	4.4364
40.0	4.5076
∞	4.5324

C' = Correction factor
d = Diameter of the polymer films
s = The distance between probes
(See section 1.8)

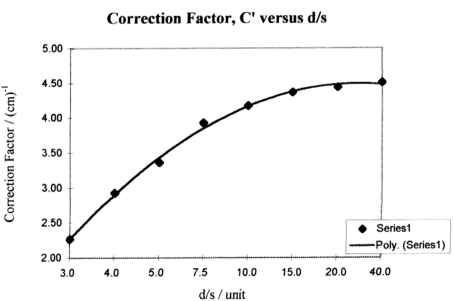

Figure 3.41 A plot of Correction factor (C') versus d/s value

3.3.3. Use of PSS of molecular weight 70,000 as dopant

There were several reasons for using lower molecular weight PSS. One is related to the solubility problem of *mw*.10^6 PSS, which dissolved only slowly in water. Another disadvantage of the higher molecular weight of PSS is that the solution produced was highly viscous. In addition, it was found that there was no significant difference in the conductivity and flexibility of the films prepared from the two types of PSS. A comparison of the surface conductivity of both dopants is showed in figure 3.42.

3.3.4. The relationship between density and surface conductivity

From figure 3.44, The surface conductivity seems to increase with the density of the films. This feature can be explained by the more compact structure of the denser films. The transportation of electron and ions in those compact films is better compared to porous films. Compact films having more conjugation polymer chains per unit volume and the conjugated system is the main contributor in the electrical conductivity.

3.3.5. Effect of total charge consumed the thickness of the film

Figures 3.45 and 3.46 show the plots of total charge used in electropolymerization versus the thickness of Ppy-PSS films. Both graphs showing the same trend. As expected higher charge was needed in order to produce thicker films.

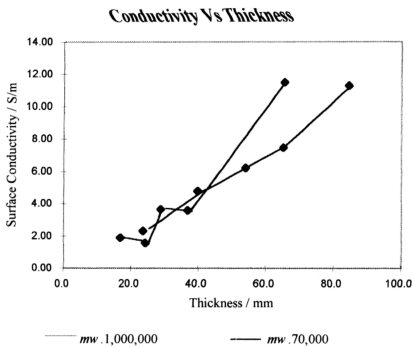

Figure 3.42 Plot showing the surface conductivity for both *mw*. 70,000 and 1,000,000 PSS at different thickness.

Table 3.9 Data for some parameters and properties of Ppy-PSS films and their surfaces conductivity

films	Thickness cm	Diameter cm	Weight g	Volume cm^3	Surface Conductivity $S\ m^{-1}$	Density $g\ cm^{-3}$
1	0.00502	1.161	0.0039	0.0053		0.734
2	0.00477	1.019	0.0059	0.0039		1.517
3	0.00650	1.344	0.0096	0.0092	7.47	1.041
4	0.00539	1.351	0.0089	0.0077	6.23	1.152
5	0.00557	1.348	0.0089	0.0079	5.00	1.120
6	0.00398	1.369	0.0056	0.0059	4.80	0.956
7	0.00236	1.368	0.0033	0.0035	2.32	0.951
8	0.00577	1.368	0.008	0.0085		0.943
9	0.00844	1.341	0.013	0.0119	11.28	1.091

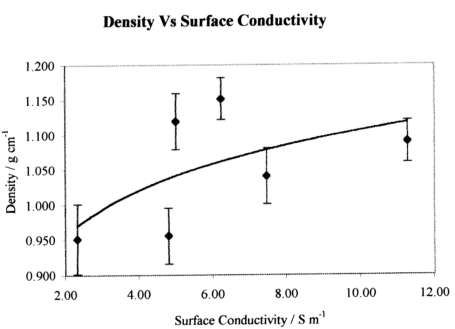

Figure 3.43 Plot showing the trend of surface conductivity when the density of the films increased.

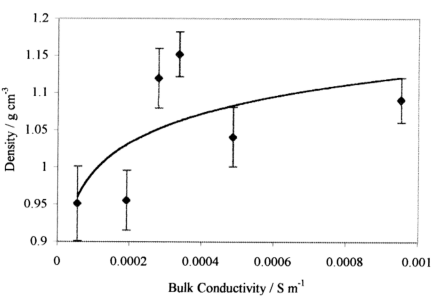

Figure 3.44 Plot showing the trend of bulk conductivity when the density of the films increased.

3.3.6. Effect of current and polymerization time on film thickness.

The thickness of Ppy-PSS films is strongly affected by the total amount of charge applied and the electropolymerization period, as mentioned in section 3.3.5. The calculation of total charge is given by:

$$\text{Total charge} = \text{current} \times \text{time}$$

$$Q = I\,t$$

Graphs of thickness versus total charge were plotted as shown in figure 3.45 and 3.46. For a given total charge used, thicker films were obtained with higher currents and shorter periods of electrolysis.

Table 3.10 : Effect of current and polymerization time on the thickness of Ppy-PSS films for *mw.*70,000 of PSS

Films	I/mA	t/min	Q/ x 10^{-3} C	Thickness/μm
1*	10/50/100	15/15/10	114	50.2
2	80	20	96	47.7
3	100	20	120	65.0
4	100	20	120	53.9
5	100	20	120	55.7
6	50	30	90	39.8
7	50	15.5	46.5	23.6
8	50/120/150	8/5/7	123	57.7
9	200	20	240	84.4
14	50	30	90	24.0
15	50	30	90	34.9

(* : 10mA for 15min followed by 50mA for 15min and 100mA for 10min)

Table 3.11 : Effect of current and polymerization time on the thickness of Ppy-PSS films for *mw.*1,000,000 of PSS

Films	I/mA	t/min	Q/ x 10^{-3} C	Thickness/μm
10a	50	15	45	24.2
11a	50	30	90	36.8
6a	50	30	90	28.8
7a	50	15.5	46.5	16.8
9a	200	20	240	65.3

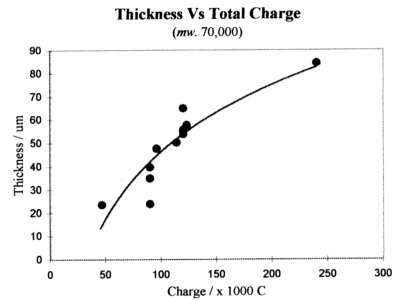

Figure 3.45 A plot showing the effect of total charge on film thickness used in electropolymerization of pyrrole with 70,000*mw.* PSS as dopant
Electrolyte :- 0.5M pyrrole + 0.5M PSS

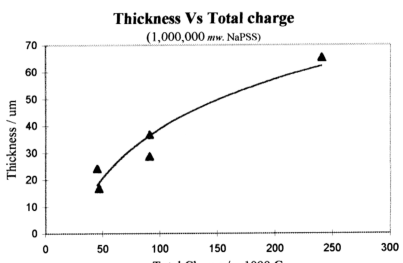

Figure 3.46 A plot showing the effect of total charge on film thickness used in electropolymerization of pyrrole with 100,000*mw.* PSS as dopant
Electrolyte :- 0.5M pyrrole + 0.5M PSS

3.4. **Conductivity across Ppy-PSS films**

Theory

The "four-point probe" method is used only for measuring surface conductivity of the films. The conductivity across the Ppy-PSS film can not be measured directly using the same method. A method using two stainless steel pellets was developed to determine bulk conductivity or cross-film conductivity. For this measurement a small current was passed through the polymer film from one side to another and the potential between the two pellets was measured (Figure 2.8).

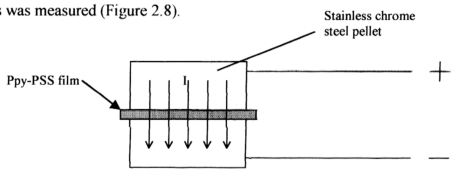

Figure 3.47 A diagram showing current flow in the bulk conductivity measurement.

The current-potential data were obtained from Cyclic Voltammetry. The typical CV for the systems is shown at figure 3.48. A linear curve was observed in the small range of potentials (±50mV). The slope of the plot represents the value of resistance. So that, the resistance for film No.14 at 1379 kPa is given by:

$$R = \text{slope}$$

$$= (3.529 \pm 0.003)\ \text{ohm}$$

A CV for the two pellets when not separated by polypyrrole films and without any applied pressure from hydraulic press is given in figure 3.49. The resistance (blank) was negligible compared to the film resistance.

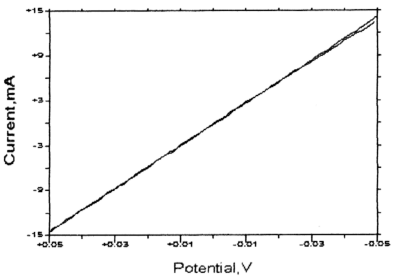

Figure 3.48 A linear plot for the film No.14 at a high pressure (1379kPa) by using the method of "two-pellet".

Gradient = $(283.1 \pm 0.3) \times 10^{-3}\ \Omega^{-1}$

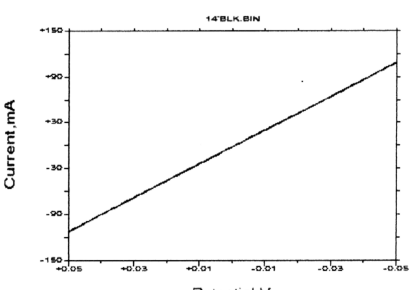

Figure 3.49 A linear plot for the two pellets without any polymer films and without any applied pressure from the hydraulic press.

Gradient = $(217.9 \pm 0.3) \times 10^{-2}\ \Omega^{-1}$

3.4.1. **Calculation for body conductivity**

For the "two-pellet" method, conductivity was calculated using the equations below:

$$\textbf{Resistance} = \mathbf{V / I} \qquad \text{.....(3.4.1 a)}$$

and, $\textbf{Resistance, } R \propto l / A$

$$R = \rho l / A$$

$$\rho = RA / l \qquad \text{.....(3.4.1 b)}$$

where, ρ = resistivity

l = the thickness of the film

A = the geometrical area cross-section of the stainless steel pellet surface

Conductivity (equation 3.3.2 b),

$$\sigma = 1/\rho$$

$$= l / RA$$

$$= (l/A) . (I/V)$$

$$= (l/A)\, m^{-1} \qquad \text{.....(3.4.1 c)}$$

where, m = V / I = slope of the graph V vs. I

error, $\delta\sigma = (\delta l / l + \delta A/A + \delta m/m) \times \sigma$

Example of calculation is given in Appendix **8**.

3.4.2. **High Pressure Effects**

The pressure-resistance data for the Ppy-PSS film No.14 is given in Table 3.14. The plot in figure 3.50 shows that the resistance for this film dropped about 80% when pressure was increased from 1379 kPa to 2758 kPa. But there was only 4% dropped for further increased in pressure from 2758 kPa to 3447 kPa and finally 5516 kPa. These results showed that the resistance decreased with the pressure reaching a limiting value. The resistance changes when the pressure was reversed from high to low were also investigated. The same result was obtained except that the resistance at 1379 kPa was lower than the previous value. (1.43 ohm compared to 3.53 ohm). The film structure appeared to have been altered after such high pressures were applied (See section 3.4.5, figure 3.65).

Another film (No.9) was compressed at pressures below 3500 kPa and the resistance-pressure plot showed a smooth curve, with decreasing gradients (Figure 3.51).

Suggested reasons why higher pressure produced lower film resistivity:

(1) The surface area of film to metal pellet contact - The "cauli-flower" peaks on the surface of Ppy-PSS had been flatten during the pressing process. The contact area was increased due to the compression. This is proved by the microscopic studies of the surface morphology as mentioned in section 3.4.

(2) A more compact film - A more compact film was expected when applying such high pressure to the film. A shorter distance for the electrons to move from one pellet to another. The transportation of electrons in a more compact Ppy-PSS film is expected to be easier.

Table 3.12 : Resistance for film No.14 at different pressure

Pressure		resistance/ohm		
/ lb/in^2	kPa	forward	reverse	Blank
200	1379	3.529	1.433	0.369
400	2758	0.692		0.369
500	3447	0.660	0.667	0.369
800	5516	0.606	0.703	0.369

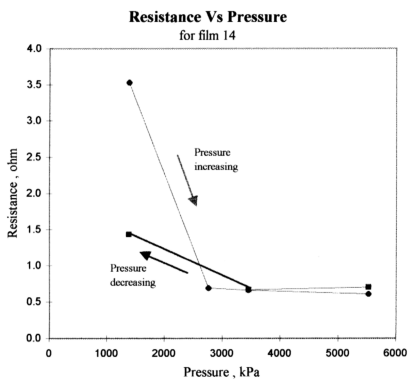

Figure 3.50 Plots showing the relationship between resistance and pressure for film No.14
(a) Pressure increasing
(b) Pressure decreasing

Table 3.13 : Resistance for film No.9 at different pressures

lbf / sq.in	kPa	R/ohms
0	0	0.752
200	1379	0.550
300	2068	0.462
400	2758	0.431
500	3447	0.422

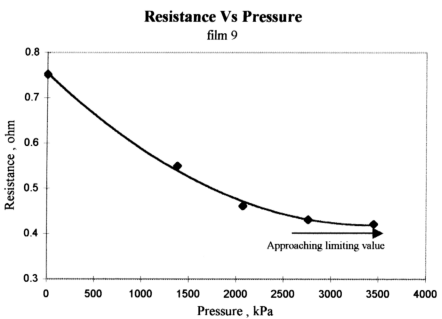

Figure 3.51 Plots showing the relationship between resistance and pressure for film No.9

3.4.3 **Low pressure (0 < P < 1000kPa)**

The effect of applying lower pressure instead of high pressure on the resistance of Ppy-PSS films was also investigated. The results are given in figures 3.52 to 3.57. Figures 3.52 and 3.53 show that resistance of the films decreased as the pressure was increased. Irreversible behaviour of the resistance was also found as shown in figures 3.54 and 3.55, when pressure was reversed.

Figure 3.56 shows a plot of Log (resistance) versus pressure for film No.14. The curve is almost linear.

Figure 3.57 is the total view of the relationship between resistivity and pressure for different films. The films 6, 9, 14, 15 possess different thicknesses. Their thicknesses are given in Table 8 with film No.14 being the thinner, followed by 6, 15 and the thickest 9. The result showed that thinner films will having higher resistivity across the films. This observation is similar to what was observed from surface conductivity measurements using the "four-point probe" method.

In figure 3.58, the film resistance is plotted over the whole range of applied pressure, and in figure 3.59 log (resistance) plotted against pressure. It is seen that above 2000 kPa the resistance reaches a limiting value. For log (R) versus pressure, linearity was observed only for pressure < 600 kPa.

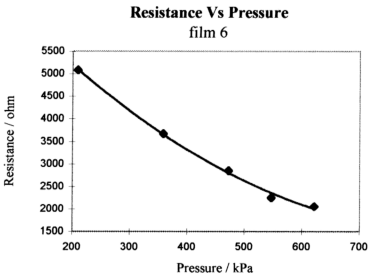

Figure 3.52 Resistance versus pressure for film No.6

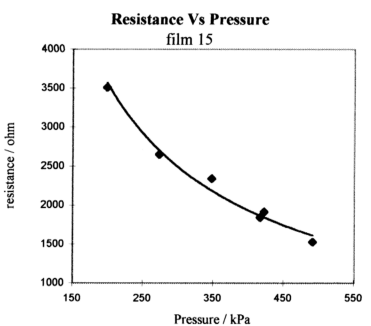

Figure 3.53 Resistance versus pressure for film No.15

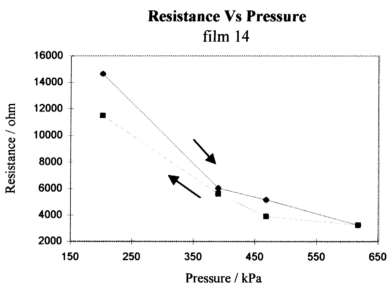

Figure 3.54 Resistance versus pressure for film No.14
The arrows showing the resistance measuring direction

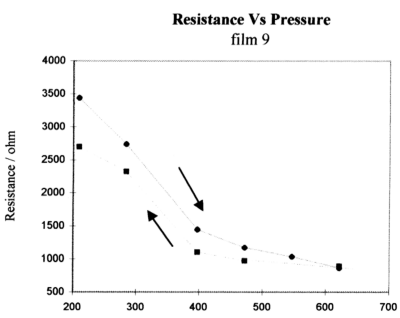

Figure 3.55 Resistance versus pressure for film No.9
The arrows showing the resistance measuring direction

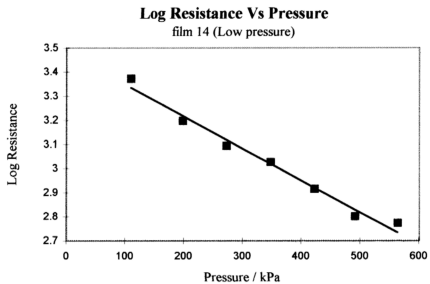

Figure 3.56 A plot showing Log(resistance) Vs pressure for film No.14 at low pressure

3.37178	110.213
3.19688	198.388
3.09457	273.022
3.02679	347.612
2.91536	422.245
2.80082	491.193
2.77203	563.734

Regression Output:

Constant	3.48138
Std Err of Y Est	0.03098
R Squared	0.98292
No. of Observations	7
Degrees of Freedom	5
X Coefficient(s)	-0.001326238
Std Err of Coef.	7.81823E-05

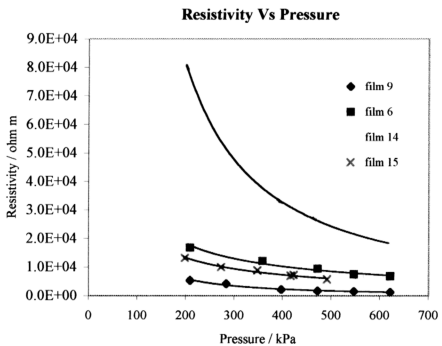

Figure 3.57 Plot showing Resistance versus Pressure for four different films

Table 3.14 : A combination of high pressure and low pressure effects to film No. 14.

wt./g	lbf / in^2	kPa	R/ohms	log R
1477.3		110	2353.837	3.372
2659.21		198	1573.557	3.197
3659.6		273	1243.269	3.095
4659.41		348	1063.619	3.027
5659.8		422	822.917	2.915
6583.98		491	632.147	2.801
7556.33		564	591.599	2.772
	200	1379	3.529	0.548
	400	2758	0.692	-0.160
	500	3447	0.660	-0.180
	800	5516	0.606	-0.218

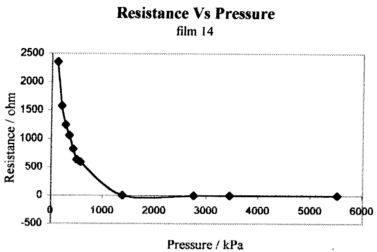

Figure 3.58 plot showing the combination of high and low pressure effects to film No. 14

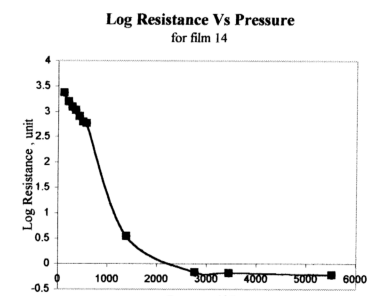

Figure 3.59 plot showing the Log (R) versus pressure for high and low pressure on film No. 14

3.4.4. AC impedance measurement on Ppy-PSS film

AC impedance measurement was carried out to compare the resistance values obtained with method of "two-pellet". Two films, sample numbers 14 and 15 were compared. The frequency range 40 to 100000 Hz was used. Figures3.60 and 3.61 show the results of AC impedance measurements on the films. From the graphs, film 14 had higher resistance (260 ohm) compared to film 15 (185 ohm). (See comparison Table 3.15).

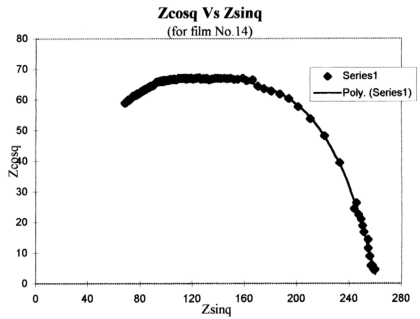

Figure 3.60 Ac impedance spectrum for film No. 14.

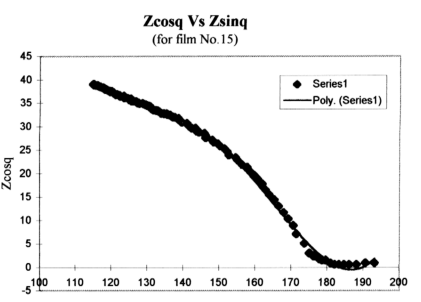

Figure 3.61 Ac impedance spectrum for film No. 15.

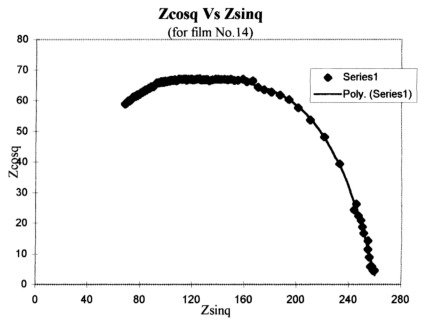

Figure 3.60 Ac impedance spectrum for film No. 14.

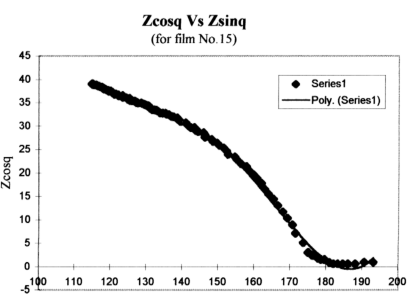

Figure 3.61 Ac impedance spectrum for film No. 15.

3.4.5. Comparison between all the three methods used in the conductivity measurement.

Table 3.15 : Comparison between three methods in the conductivity of films 14 and 15

Film	Thickness, μm	Bulk Conductivity by "AC impedance", Sm^{-1}	Bulk Conductivity by "four-point probe" Sm^{-1}	Bulk Conductivity by "two-pellet" Sm^{-1}	
				High Pressure	Low Pressure
14	24.0	2.04×10^{-4}	2.52×10^{-5}	5.17×10^{-2} to 3.01×10^{-1}	1.25×10^{-5} to 5.61×10^{-5}
15	34.9	4.29×10^{-4}	5.06×10^{-5}	3.42×10^{-1} to 4.15×10^{-1}	7.54×10^{-5} to 1.74×10^{-4}

From table 12, the bulk conductivity of films 14 and 15 were compared. The bulk conductivities by "four-point probe" were obtained from multiplication of surface conductivity and the film thickness. The value of conductivity by "AC impedance" was ten times greater than the conductivity obtained from "four-point probe". The bulk conductivity, in the "low pressure" application, was in the range of the method of "four-point probe". In the "high pressure" application, the bulk conductivity was found to be 10^3 and 10^4 greater than conductivities obtained from the other two methods.

For the three methods described above, film 14 which was thinner than film 15 shows lower bulk conductivity. Although there is agreement showing that the thicker films possess higher conductivity, further study is needed to asccertain what are the correct values of bulk conductivity.

3.4.6. Microscopy study of the Ppy-PSS surface after compression

Figures 3.63 and 3.64 showed a part of a Ppy-PSS surface (magnification 1000x) before the high pressure was applied. The "cauli-flower" or dome type of structure was found. The flattening of "domes" was observed after hydraulic compression at high pressure for few minutes (Figure3.65). A schematic diagram represents the change before and after pressure treatment is shown below:

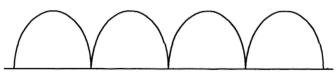

before pressing

after pressing

Figure 3.62. A diagram showing the difference in surface structure of Ppy-PSS before and after pressing.

This could explain the irreversible behaviour of resistance on reversing pressure on the films.

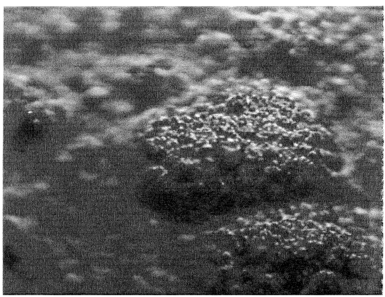

Figure 3.63 A picture of Ppy-PSS surface growth on electrolyte side. Image by using Leica Q500MC image Processing and Analysis system.
1000X magnification

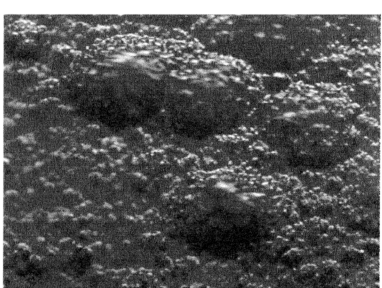

Figure 3.64 A picture of Ppy-PSS surface growth on electrolyte side. Image by using Leica Q500MC image Processing and Analysis system.
1000X magnification

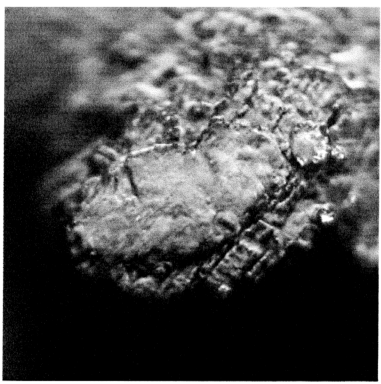

Figure 3.65 A picture of Ppy-PSS surface which taken after a high pressure was applied. Image by using Leica Q500MC image Processing and Analysis system. 1000X magnification.

3.4.7. **Platinised Titanium**

The surface of a titanium piece, after polishing with emery paper, is shown in figures 3.66 and 3.67. After platinization the surface became smoother. The whole titanium surface was covered by platinum particles evenly (Figure 3.68). The fresh deposited platinum was very electroactive but did not adhere strongly on to titanium surface.

A way to increase the adhesion of platinum particles to the titanium surface is through sintering. The sintered platinised titanium plate appeared darker (Figure 3.69). The electrocatalytic activity of sintered PT was found to be as good as pure Pt (see section 3.1.7).

Figure 3.66 A picture of Sulphonated polyaniline coated Ppy-PSS surface. Image by using Leica Q500MC image processing and analysis system. 1000X magnification.

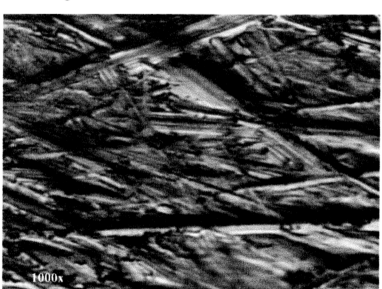

Figure 3.67 A picture of Sulphonated polyaniline coated Ppy-PSS surface. Image by using Leica Q500MC image processing and analysis system. 1000X magnification.

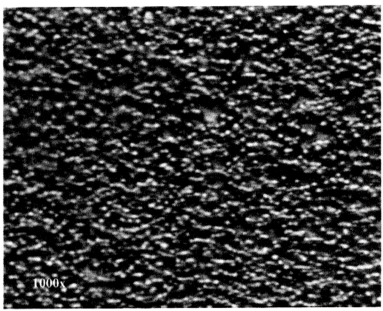

Figure 3.68 A micropicture of Platinised Titanium surface before sintering. Image by using Leica Q500MC image Processing and Analysis system. 1000X magnification.

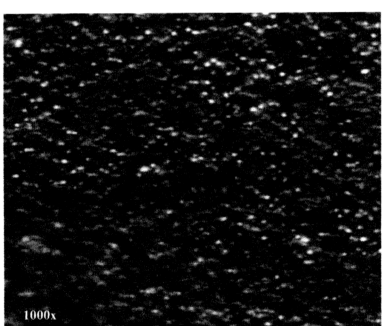

Figure 3.69 A micropicture of Platinised Titanium surface after sintering. Image by using Leica Q500MC image Processing and Analysis system. 1000X magnification.

3.5 **Copper removal**

3.5.1. Cyclic Voltammetry study

Cyclic Voltammetry was used to investigate the ion-exchange process between Ppy-PSS film and Cu^{2+} and copper deposition/reduction on the cathodic film (electrode). With a Ppy-PSS film as working electrode, cyclic potential (w.r.t. Ag/AgCl) scans were carrid out between +300mV to −1000mV. The C V is shown in figure 3.70. A reduction peak was observed and this was believed to be due to the copper deposition.

The copper was being electrodeposited on the Ppy-PSS surface. This was indicated by the colour change of the area exposed to the electrolyte from black to brown, which is the colour of copper metal.

The peak height in terms of current value was increased when a sample solution containing higher concentration of Cu^{2+} was used. Figures 3.71 and 3.72 show CV's for three different concentrations, 33, 157 and 307 ppm of Cu^{2+}.

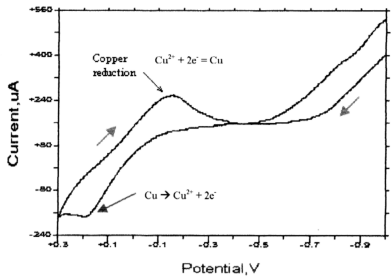

Figure 3.70 Cyclic Voltammetry for Ppy-PSS film using 307ppm Cu^{2+} solution as electrolyte.

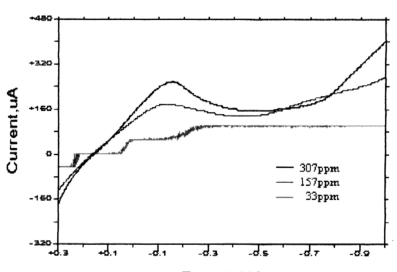

Figure 3.71 CV showing the reduction peaks at different concentration of Cu^{2+}
Working electrode: - Ppy-PSS
Number of sweeps: - 2nd

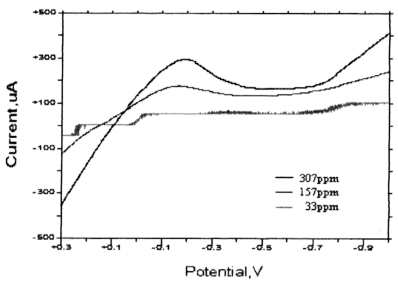

Figure 3.68 CV showing the reduction peaks at different concentration of Cu^{2+}
Working electrode: - Ppy-PSS
4^{th} sweep; -0.3V → -1.0V

3.5.2. The used of Titanium plate as substrate support for the conducting polymer in ion-removal process.

It was found that titanium could be used in the preparation of the conducting Ppy-PSS films. It is also cheaper to use than Pt and PT. There were difficulties in using the free standing Ppy-PSS films for copper ions removal. The main problem lies in forming good electrical contact between film and connectors. As the free standing films were generally brittle, they tend to be broken by the electrical contact clips

Adhesion of Ppy-PSS on Titanium surface was strong enough to give a good electrical contact between metal and conducting polymer films. The contact clip was attached to the titanium support plate (See diagram in figure 3.69).

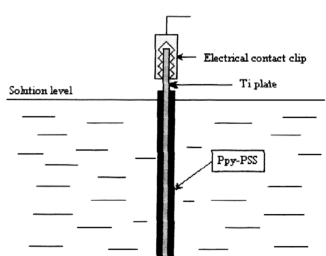

Figure 3.69 A diagram showing Titanium as supporting substrate in the copper removing process

3.5.3. Copper removal by ion-exchange / deposition by alternately depositing and stripping using Ppy-PSS film

The original objective for this part of project was to apply a cathodic potential to the conducting and sulphonated Ppy-PSS film in order to reduce the Cu^{2+} on the surface of the film or to enhance Cu^{2+} ion exchange process. The film was then taken out of the sample solution and dipped in a small volume of electrolyte and an anodic potential applied to it to allow the copper to re-dissolve. This process of transferring Cu^{2+} from a big volume sample solution to a small volume of electrolyte was actually concentrating the Cu^{2+}. But the platted copper was found to be easily dissolved in dilute sulphuric acid solution (0.01M) even without applying an anodic potential. Though this test was applied for simulated dilute Cu^{2+} effluent, it could be applicable to recovery of other heavy metals using the same technique.

A fixed potential -400mV was applied to the system. Cu ions were being attracted to the film surface. The exchange process occurred followed by the reduction of Cu^{2+} and deposition on the polymer film. After that the copper was deposited on copper itself. The colour of the film initially changed from black to blue before turning brown. However, the deposition of copper was not evenly distributed throughout the working electrode. The deposition occurred more rapidly on the edges. This feature might be due to poor throwing power and unequal distribution on the whole surface of working electrode.

The blue colour was probably caused by the concentration of Cu^{2+} due to the attraction of Cu^{2+} ions to the working electrode. Figures 3.74 and 3.75 show the uneven deposition of copper and the colour difference due to copper ions and metallic copper. The shiny copper turned dark and finally greenish after it was left in moist atmosphere

overnight. The dark colour material was probably copper oxide and the greenish form was actually hydroxo carbonate, due to corrosion.

The copper deposited at the surface of Ppy-PSS was easily removed by dipping the film in a small volume (25mL) of dilute sulphuric acid (0.01M). The total surface area of conducting Ppy-PSS was (22.0 ± 0.2) cm^2 (both sides) and the volume of sample Cu^{2+} solutions was (70.0 ± 0.5) mL. So, the total surface area per unit volume was:

$$\text{Total area per unit volume} = (22/70)\ cm^{-1}$$

$$= (0.31 \pm 0.01)\ cm^{-1}$$

The whole process could be described as:

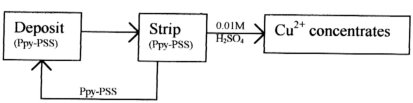

Figure 3.76 A diagram showing steps in copper removal processes.

Figures 3.77 and 3.78 show the decreasing of the copper concentration in sample solutions versus time.

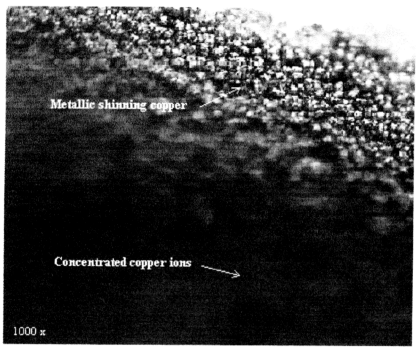

Figure 3.74 A picture of deposition copper image on the Ppy-PSS surface obtained by using Leica Q500MC image processing and analysis system. 1000X magnification.

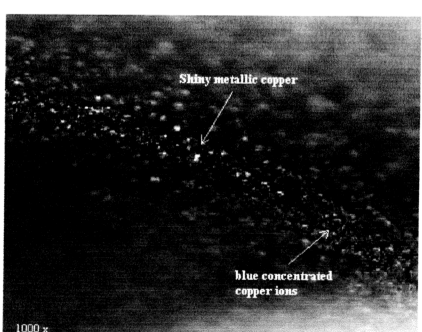

Figure 3.75 A picture of deposition copper image on the Ppy-PSS surface obtained by using Leica Q500MC image processing and analysis system. 1000X magnification.

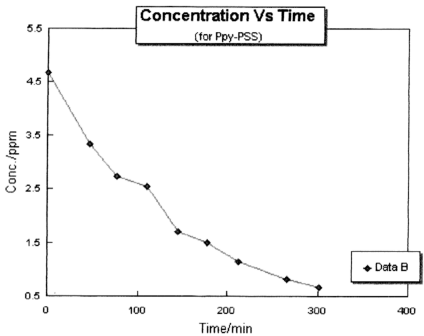

Figure 3.77 A plot showing the removal of copper ions using conducting Ppy-PSS
Surface area per unit volume : 0.314cm^{-1}.
Working electrode :- Ppy-PSS on Ti
Voltage = 400 mV Current = 2 to 70 mA

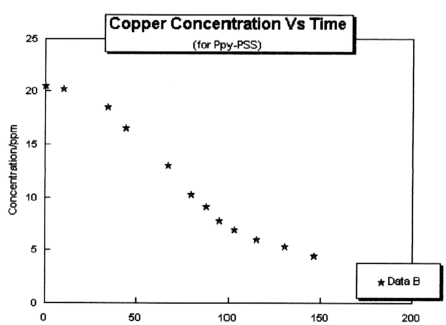

Figure 3.78 A plot showing the removal of copper ions by using conducting Ppy-PSS
Surface area per unit volume : 0.314cm^{-1}; Working electrode :- Ppy-PSS on Ti
Voltage = 400 mV Current = 2 -70 mA

3.5.4. Continuous deposition without stripping.

This test was carried out in order to determine whether the copper in solution could be totally removed by continuous deposition on the polymer surface. The results showed that the amount of copper deposited on the Ppy-PSS surface reached a limiting situation where the copper re-dissolved into the sample solution. Figure 3.79 shows that copper was being removed during first 40 min with concentration decreasing, but the concentration of Cu^{2+} in sample solution increased again after about 60 to 70 min.

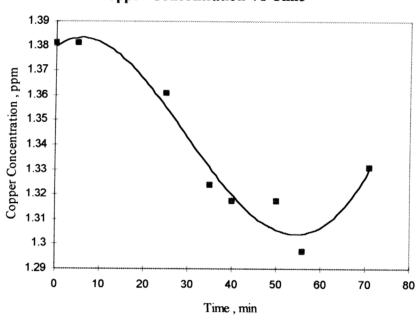

Figure 3.79 A plot showing the removal of copper ions using conducting Ppy-PSS without stripping.
Surface area per unit volume : $0.314cm^{-1}$.
Working electrode :- Ppy-PSS on Ti
Voltage = 400 mV Current = 2 to 70 mA

3.5.5. Using the Ppy-PSS/Pan composite film

A double layer conducting film was prepared and tested for copper removal. One layer was Ppy-PSS and an additional layer of sulphonated polyaniline (PAN) was coated on the Ppy-PSS surface. Although the powder form of PAN on the Ppy-PSS was easily washed off but a very thin PAN layer remained which was more adhesive. The green colour of PAN could still be observed. The surface structure was investigated with the Leica microscope and the image is given in Figure 3.80.

The copper removing function of the Ppy-PSS/PAN (Figure 3.82) film was compared to the original Ppy-PSS film (Figure 3.81) and the combination of both as shown at figure 3.83. The starting concentration of samples used was not much different for the purposed of comparison. The results showed no significantly improvement on the removal of copper. This was expected due to the little amount of sulphonated PAN on the surface of Ppy-PSS.

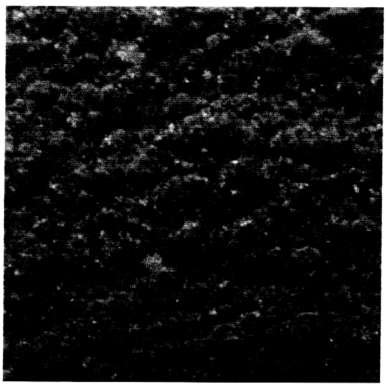

Figure 3.80 A picture of sulphonated polyaniline coated Ppy-PSS surface. Image by using Leica Q500MC image processing and analysis system. 1000X magnification.

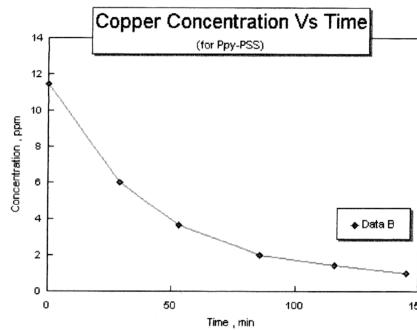

Figure 3.81 A plot showing the copper ions removing process by using conducting Ppy-PSS
Surface area per unit volume : $0.314cm^{-1}$.
Working electrode :- Ppy-PSS on Ti

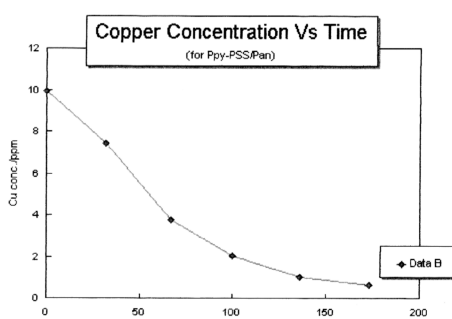

Figure 3.82 A plot showing the copper ions removing process by using conducting Ppy-PSS/PAN
Surface area per unit volume : $0.314cm^{-1}$.
Working electrode :- Ppy-PSS on Ti

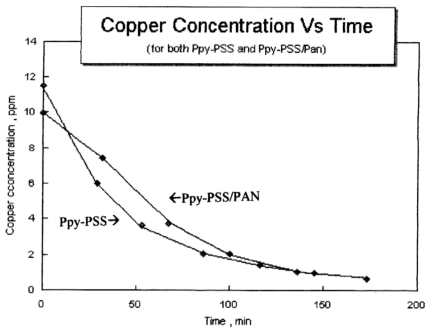

Figure 3.83 A plot showing the copper ions removing process by using conducting Ppy-PSS
Surface area per unit volume : $0.314cm^{-1}$.
Working electrode :- Ppy-PSS on Ti